Catal Lett (2009) 130:154–160
DOI 10.1007/s10562-009-9842-0

Studies on Ceria Supported Vanadium Incorporated Ammonium Salt of 12-Molybdophosphoric Acid Catalysts

K. Mohan Reddy · N. Lingaiah · P. S. N. Rao · P. Nagaraju · P. S. Sai Prasad · I. Suryanarayana

Received: 1 October 2008 / Accepted: 6 January 2009 / Published online: 4 February 2009

Abstract A series of ceria supported vanadium incorporated ammonium salt of 12-molybdophosphoric acid (AMPV) catalysts were synthesized in a single-step by generating Keggin structure in situ. These catalysts were characterized by X-ray diffraction, FT-infrared, BET surface area, thermal analysis (TG/DTA) temperature programed reaction and acidity by potentiometric titration. The catalytic activities of these catalysts were tested for the vapor phase ammoxidation of 2-methylpyrazine to 2-cyanopyrazine. The CeO_2 supported AMPV catalysts are more active and selective compared to other supports. The high activity and selectivity of these catalysts are related to the presence of both redox vanadium and oxygen storage release function of ceria.

Keywords 12-Molybdophosphoric acid · Vanadium · Ceria · Ammoxidation · 2-Methylpyrazine · 2-Cyanopyrazine

1 Introduction

Heteropoly acids with Keggin structure are important class of catalysts due to the possibility of controlling their acidic and redox properties that allows to design at atomic-molecular level [1–3]. The main constrain to use these materials for heterogeneous gas phase reactions are due to their low surface area and less thermal stability [4]. A convenient way to use these solids for gas phase reactions is to disperse these in matrixes on solid supports such as silica, titania and carbon, which enhances their specific surface area and thermal stability. The acidic and redox properties of heteropoly acids can be tuned by the partial substitution of Mo with transition metal like V [5–7].

Ammoxidation refers to interaction ammonia with reducible organic compounds [8] for the preparation of industrially important nitriles, which are used in the preparation of dyestuffs, pesticides and pharmaceuticals. For this reaction the catalyst should posess acidic and redox functionalities [9]. Vanadia based catalysts are extensively studied for various ammoxidation reactions [10–12]. However, these catalysts show low nitrile selectivity due to over oxidation [13].

The support used to disperse the active component plays an important role for ammoxidation reaction, as it is responsible for the formation of acid–base and redox centers on the surface of the catalyst [14]. The most significant one among those oxides is CeO_2. Because of its ability to store and release of oxygen it undergoes exist in the redox states (Ce^{+4} and Ce^{+3}) under reaction conditions is useful for this reaction [15]. Recent investigations reveal that CeO_2 supported V_2O_5 catalysts exhibited good catalytic activity for partial oxidation of methanol to formaldehyde [16, 17]. Bart et al. [18] studied the cerium based mixed oxides in the ammoxidation of propylene. Vanadium containing heteropoly acids supported on different metal oxides are widely studied, however, no detailed studies are available on the preparation and evaluation of either vanadium incorporated heteropoly acids or their salts supported on ceria. It is quite obvious that the combination of vanadia (known for its redox properties) and ceria (known for its oxygen storage and release functions) can

K. Mohan Reddy · N. Lingaiah · P. S. N. Rao · P. Nagaraju · P. S. Sai Prasad · I. Suryanarayana (✉)
Inorganic and Physical Chemistry Division, Indian Institute of Chemical Technology, Hyderabad 500 607, India
e-mail: iragavarapu@iict.res.in

N. Lingaiah
e-mail: nakkalingaiah@iict.res.in

Scheme 1 Generalized reaction scheme of ammoxidation of 2-methylpyrazine

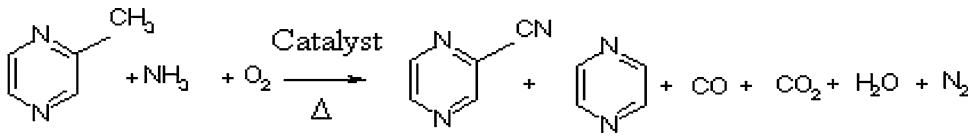

give rise to a better catalytic system for ammoxidation reaction.

In the present investigation, an attempt is made to synthesize the Keggin ion of vanadium incorporated ammonium salt of molybdophosphoric acid on ceria in a single step. These catalysts were characterized in order to understand the stability of ammonium salt when vanadium is incorporated into the Keggin structure. The catalytic activities of these catalysts were evaluated for the ammoxidation of 2-methylpyrazine (MP) to 2-cyanopyrazine (CP) (Sch. 1), which is an important step in the synthesis of pyrazinmide, an anti TB drug.

2 Experimental

2.1 Catalyst Preparation

Ceria supported vanadium incorporated ammonium salt of 12-molybdoposphoric acid (AMPV) catalysts with 5–25wt% loading were prepared by impregnation method. A mixture of required quantities of aqueous solutions of ammonium heptamolybdate, ammonium metavanadate (such that the Mo/V atomic ratio 11/1) and diammonium hydrogen orthophosphate were dissolved in minimum amount of water. This solution was first refluxed at 100 °C for 6 h and then the required quantity of this solution was added to the support, generating the Keggin ion in one step. After the addition of this solution to support, the pH of the solution was adjusted to 1 by adding dilute HNO_3. The excess solution was evaporated on water bath and dried in oven at 120 °C for 12 h. Finally these catalysts were calcined in air at 350 °C for 4 h. The other supported (AlF_3, SiO_2, TiO_2 and ZrO_2) catalysts are also prepared in a similar manner. Here after these catalysts are designated as 5–25% AMPV/CeO_2.

2.2 Catalyst Characterization

X-ray diffraction (XRD) patterns of the catalysts were recorded on a Rigaku Miniflex diffractometer using CuK_α radiation. FTIR spectra were recorded on a DIGILAB (USA) spectrometer, with a resolution of 1 cm^{-1} using KBr disc method. The BET surface areas of the catalyst samples were calculated from N_2 adsorption–desorption data acquired on an autosorb-1 instrument (Quantachrome, USA) at liquid N_2 temperature. The powders were first outgassed at 120 °C to ensure a clean surface prior to construction of adsorption isotherm. The TGA/DTA analysis was carried out on a Mettler–Toledo apparatus. With a sample weight of ca. 30–40 mg, the tests were performed under nitrogen flux in the temperature ranging from 25 to 800 °C and at a heating rate of 10 °C/min. Temperature programmed reduction (TPR) of the catalysts were carried out in a flow of 10% H_2/Ar mixture gas at a flow rate of 30 mL/min with a temperature ramp of 10 °C/min. Before the TPR run the catalysts were pretreated with argon at 300 °C for 2 h. The hydrogen consumption was monitored using a thermal conductivity detector.

The acidity of the solid samples was measured by the potentiometric titration method. A known amount of catalyst sample suspended in acetonitrile was stirred for 3 h and then the suspension was titrated with a solution of 0.05 N *n*-butyl amine in acetonitrile, at a flow rate of 0.05 mL/min. The variation in the electrode potential was measured with an instrument having a digital pH meter, (Automatic titrator, Schott GmbH, Germany) using a standard calomel electrode. The potentiometric titration was performed with a glass electrode. The instrument was calibrated using standard buffer solutions. The acidity of the catalysts measured by this technique enables determination of the total number of acid sites and their strength [19].

2.3 Catalytic Reaction

Ammoxidation of MP was carried out in a micro reactor at atmospheric pressure in the temperature range of 360–420 °C. In a typical experiment about 3 g of the catalyst mixed with 3 gm of quartz beads (18/25 BSS size) and loaded in the reactor by suspending it in between two quartz wool plugs. The feed with a molar ratio of MP:water:ammonia:air = 1:13:7:38 was fed into the preheater portion of the reactor. The aqueous mixture of MP was metered using a microprocessor based feed pump (B. Braun, Germany), at a flow rate of 2 mL/h. After allowing the catalyst to attain steady state at each reaction temperature, the liquid product was collected for 30 min and analyzed by gas chromatography, separating it on an SE-30 column (2 m long, 3 mm diameter) using an FID detector. The reproducibility of product distribution by GC was about ±2%. From the analysis of non-condensable mixture, it was ensured that the quantity of any organic species was negligible in the exit gas. The conversion was

calculated based on the disappearance of MP and the selectivity to CP was calculated as follows:

$$S_{cp} = (CP_o \times 100)/(MP_i - MP_o)$$

where CP_o and MP_o are the amounts of 2-cyanopyrazine and 2-methylpyrazine, respectively, detected at the reactor outlet (in moles) and MP_i is the initial amount of 2-methylpyrazine (in moles). S_{cp} is the selectivity to 2-cyanopyrazine.

3 Results and Discussion

3.1 Bet Surface Area

The surface areas and acid strength values of the ceria supported AMPV catalysts are shown in Table 1. The surface area of pure CeO_2 is 45 m^2/g. The surface area values decreased with increase in AMPV loading on CeO_2. This may be due to the blockage of some pores by active component or formation of some new compounds, which are of low surface area by solid reaction between support and active species [20–22]. The elemental analyses of the studied catalysts are compared with ammonium salt of molybdophosphric acid (AMPA). The Mo/P ratio of AMPA catalyst was 12.4. The Mo/P and V/P ratio of synthesized AMPV catalyst is 11.1 and 0.93, respectively. The pure AMPV catalyst consist slightly lower contents of Mo in the Keggin units due to the partial substitution of Mo by V. The Mo/P ratios for CeO_2 supported 5–25wt% AMPV catalysts are 10.4, 10.7, 10.95, 11.10 and 11.0, respectively.

3.2 Powder X-ray Diffraction Studies

XRD patterns of the bulk and supported catalysts are shown in Fig. 1. The bulk AMPV showed the Keggin ion formation [23]. It suggests that the support exhibited strong diffraction peaks related to the cubic phase of CeO_2. The distinct fluorite oxide phase of CeO_2 is seen in all of the samples [JCPDS 34-0394]. However, the catalysts with low AMPV loading (5–10%) did not reveal any diffraction peaks related to crystalline AMPV. The absences of XRD patterns suggest the well-dispersed nature of AMPV species on CeO_2 surface. The catalysts with high AMPV loadings (15–25%) clearly exhibited the Keggin ion [24] of AMPA on CeO_2 surface. The intensity of crystalline AMPV Keggin ion peaks increased with increase in AMPV loading. Thus, the XRD data hints the amorphous nature of active species at low loadings of AMPV and presence of crystalline Keggin ions at higher loadings.

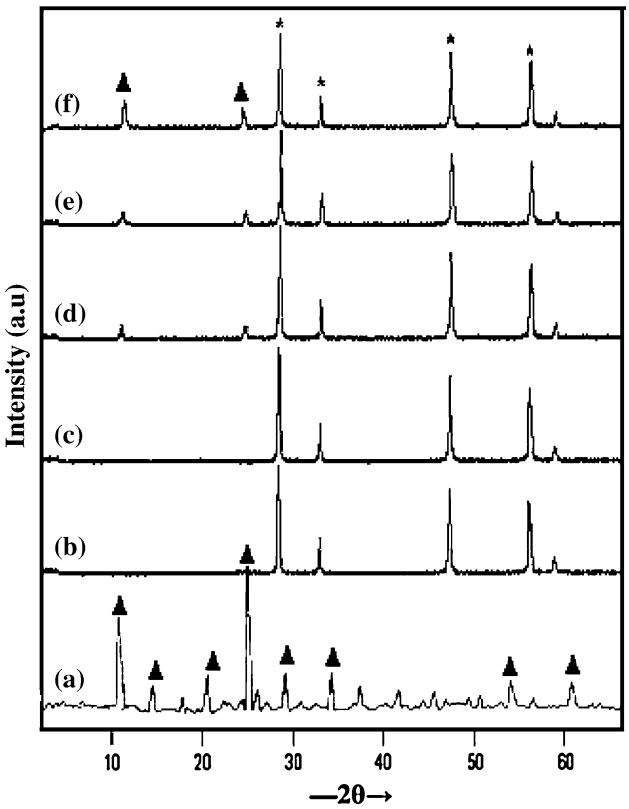

Fig. 1 XRD patterns of AMPV/CeO_2 catalysts (*a*) Bulk AMPV (*b*) 5% (*c*) 10% (*d*) 15% (*e*) 20% (*f*) 25%; (▲) Keggin ion (*) CeO_2

Table 1 BET surface area and acid strength values of CeO_2 supported AMPV catalysts

Catalyst	BET surface area (m^2/g)	Acid strength E_i (mV)
CeO_2	45	246
Bulk AMPV	50	746
5% AMPV/CeO_2	9.2	500
10% AMPV/CeO_2	7.4	532
15% AMPV/CeO_2	6.1	595
20% AMPV/CeO_2	5.3	628
25% AMPV/CeO_2	3.4	620

3.3 Fourier Transform Infrared Studies

The FT-IR spectra of the catalysts are shown in Fig. 2. Pure CeO_2 did not show any IR bands. The supported catalysts exhibit IR bands centered at 1065, 970, 873 and 790 cm^{-1}, which are assigned to stretching vibrations of NH_4^+ ion (P–O_d), (Mo–O_t), (Mo–O_b–Mo), and (Mo–O_c–Mo), of Keggin unit, respectively [23]. The bands corresponding to Keggin ion are less intense (weak) for the catalysts with low AMPV loadings (5–10%) indicates that the AMPV is highly dispersed on CeO_2. The increase in the intensity of Keggin unit bands is noticed with increase in loading suggests the crystalline nature of AMPV. The catalysts with 20 and 25% of AMPV the Keggin unit bands are shifted to lower wave number region ($\leq$5 cm^{-1}) indicating the incorporation of

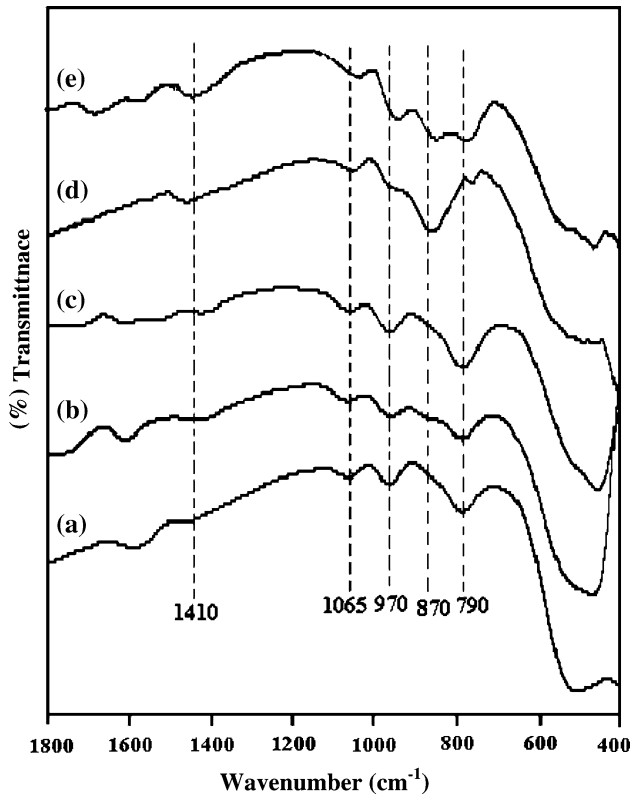

Fig. 2 FT-IR patterns of AMPV/CeO_2 catalysts (*a*) 5% (*b*) 10% (*c*) 15% (*d*) 20% (*e*) 25%

vanadium in Keggin unit. Bardin and Davis reported a shift of about 4 cm^{-1} in the P–O and Mo–O bands of $H_4PMo_{11}VO_{40}$ [25]. FT-IR analysis also suggests the formation of Keggin unit on CeO_2 surface during the single step synthesis of these catalysts.

3.4 Thermogravimetric/Differential Thermal Analysis Studies

All the supported catalysts showed similar TG/DTA patterns (Fig. 3) with two-stage weight loss at about 250 and 450 °C. Initial weight loss was noticed in the temperature range of 150–350 °C in TGA curve. The corresponding DTA peak is centered at 250 °C due to the thermal loss of constitutional water. The second stage of weight loss appeared in the temperature range of 450–470 °C, which is ascribed to the crystallization of the oxides resulting from the decomposition of the Keggin unit. As the loading was increased from 5 to 25%, the endothermic peak (450 °C) slightly shifted to higher temperature, indicating the interaction between salt and the support. The bulk AMPV catalyst showed endothermic peaks at 200 and 410 °C, due to loss of constitutional water and decomposition of Keggin ion, respectively [26]. These findings are inline with those of Bruckman et al. [27] and Marchal-Roch et al. [28] who studied the thermal behavior of supported

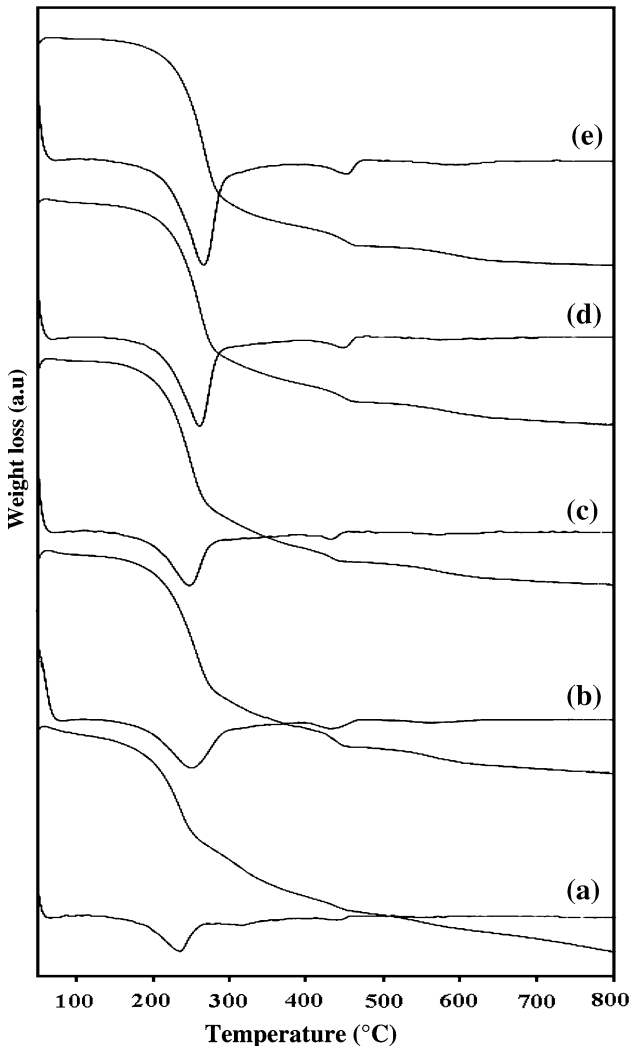

Fig. 3 TG/DTA profiles of AMPV/CeO_2 catalysts (*a*) 5% (*b*) 10% (*c*) 15% (*d*) 20% (*e*) 25%

vanadium incorporated MPA and ammonium salt of MPA. Thus, The TG/DTA studies clearly indicate that, the supported AMPV catalysts are thermally more stable compared to bulk AMPV catalyst.

3.5 Temperature Programmed Reduction Studies

TPR patterns of CeO_2 supported AMPV catalysts are shown in Fig. 4. Pure CeO_2 showed two reduction peaks around 550 and 900 °C, which are attributed to the reduction of surface Ce^{4+} to Ce^{3+} and bulk CeO_2 [29]. Addition of 5% AMPV to the support there is no drastic change in the reduction of CeO_2 except appearance of a new reduction peak at about 290 °C. Li et al. [30] have reported for vanadium substituted Cs salts of heteropoly acids and concluded that the peaks below 500 °C can be ascribed to the reduction of transition metal cations in the primary structure of heteropoly acids. Therefore, this

reduction peak may be attributed to the reduction of vanadium species present in Keggin ion. When the loading was increased to 10%, the reduction of surface CeO_2 disappeared and reduction of bulk ceria appeared at low temperature region. Interestingly, the reduction peak of vanadium species shifted to high temperature mainly because, vanadium may come out of the framework and forms vanadyl species in the secondary structure of Keggin ion during TPR analysis [31]. The reduction of these vanadyl species generally takes place relatively at high temperature. The peak observed at about 700 °C, is attributed to the reduction of free metal oxides originating from the decomposition of Keggin oxoanion [30]. With the increase in loading from 10 to 25%, similar reduction patterns are noticed except a marginal shift in reduction temperature to higher values. This is mainly because the manifestation of strong salt and support interactions.

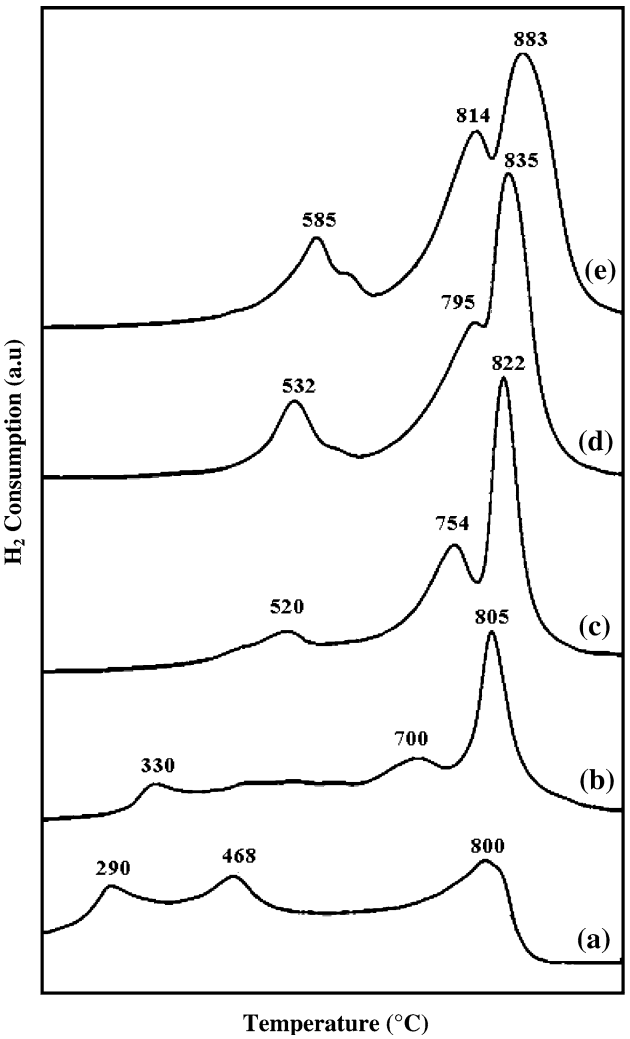

Fig. 4 TPR patterns of AMPV/CeO_2 catalysts (*a*) 5% (*b*) 10% (*c*) 15% (*d*) 20% (*e*) 25%

3.6 Acidity by Potentiometric Titrations

The acidity of catalysts was determined by potentionmetric titration method. The initial EMF (E_i) values (shown in Table 1) are taken as a measure for the acid strength of the catalysts [32]. Based on initial E_i values the strength of the acid sites are classified into the following range: $E > 100$ mV (very strong sites); $0 < E > 100$ mV (strong sites); $-100 < E < 0$ mV (weak sites) and $E < -100$ mV (very weak sites). The support CeO_2 has low acid strength and impregnation of AMPV on CeO_2 the acid strength is increased. The E_i value increased from 246 to 500 mV with the addition of 5% AMPV on CeO_2. The acid strength is futher increased with increase in AMPV loading and reached a maximum value at 20% of AMPA. Above this loading, the E_i value decreased marginally. This decrease is attributed to the bulk nature of AMPV on CeO_2.

3.7 Ammoxidation of 2-Methylpyrazine

In the ammoxidation of MP leads to produce cyanopyrazine, pyrazine, H_2O and carbon oxides. In the present study it is observed the formation of CP, pyrazine as major products. The ammoxidation activity and selectivity patterns of the catalysts, as a function of AMPV loading at different reaction temperatures are shown in Fig. 5. The

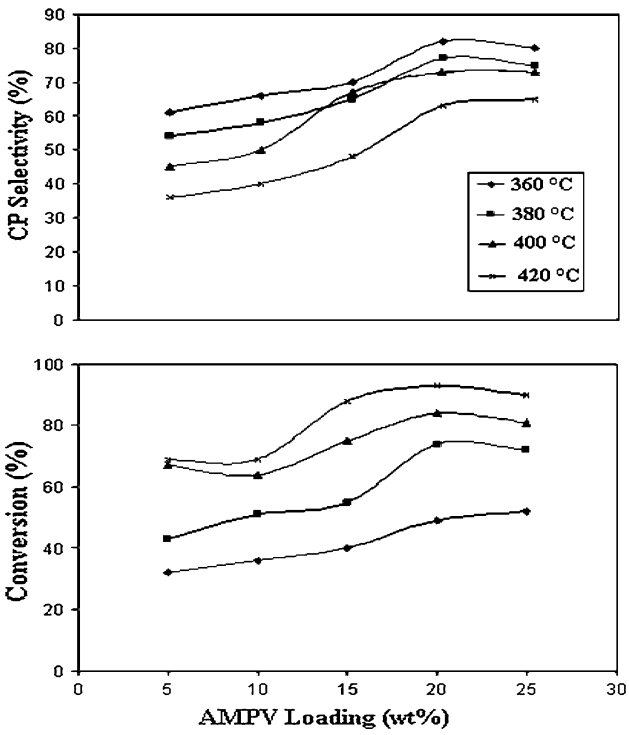

Fig. 5 Product distribution of MP in the ammoxidation reaction as a function of AMPV loading on CeO_2 at different reaction temperatures (%) transmittnace

conversion of MP increased with increase in the APMV loading and reached a maximum at a loading of 20%. The conversion remains almost constant above this loading. These results indicate that the activity was maximum for the catalyst for which the active AMPV species are well dispersed on CeO_2. It is well known that the elimination of diffusion resistance is difficult in the ammoxidation reaction, as expressed by Forni [33]. The conversion levels also increased with increase in reaction temperature from 360 to 420 °C.

The selectivity to CP also increased with increase in AMPV loading. The maximum selectivity to CP (85%) was obtained on 20% AMPV catalyst. However, the selectivity to CP is not the same as conversion when the reaction temperature increased from 360 to 420 °C. As the conversion increases the selectivity to CP decreased and the undesired dealkylated product (pyrazine) is formed. It is expected that at high temperatures oxidative dealkylation of MP will be prominent, thus leading to pyrazine formation. The activity and selectivity patterns for the best catalyst (20% AMPV/CeO_2) at various reaction temperatures suggest that about 78% conversion, and 76% selectivity was obtained at optimized reaction condition.

The comparison of the present work is made in terms of activity and selectivity with the AMPV catalysts supported on different supports (Table 2). The activity and selectivity of different supports are obtained in the following order: AMPV/CeO_2 > AMPV/SiO_2 > AMPV/TiO_2 > AMPV/ZrO_2 > AMPV/AlF_3. The better activity of CeO_2 supported catalyst was due to the presence of V and CeO_2. Vanadium, which is known for its redox properties, is responsible for high activity and selectivity of the catalysts. Oxidation reactions on vanadium occurs by a redox reaction normally followed by the Mars-Van Krevelen mechanism that employs lattice oxygen for the oxidation of the organic substrate and the gas phase oxygen supplements the loss of lattice oxygen. The lattice oxygen plays an important role in the oxidation and reduction cycle of V during the ammoxidation reaction. As ceria is known for its oxygen storage and release functionality, favors the vanadium redox functionality by releasing oxygen thereby over all ammoxidation activity is enhanced. Thus the combination of vanadium and ceria can be considered as the better catalytic system for this reaction.

Table 2 Conversion and selectivity values of 20% AMPV on different supports at 380 °C

Catalyst	Conversion of MP (%)	Selectivity to CP (%)	Acid strength (E_i)
20% AMPV/AlF_3	58	50	610
20% AMPV/ZrO_2	62	48	458
20% AMPV/TiO_2	82	66	591
20% AMPV/SiO_2	96	54	730
20% AMPV/CeO_2	72	80	628

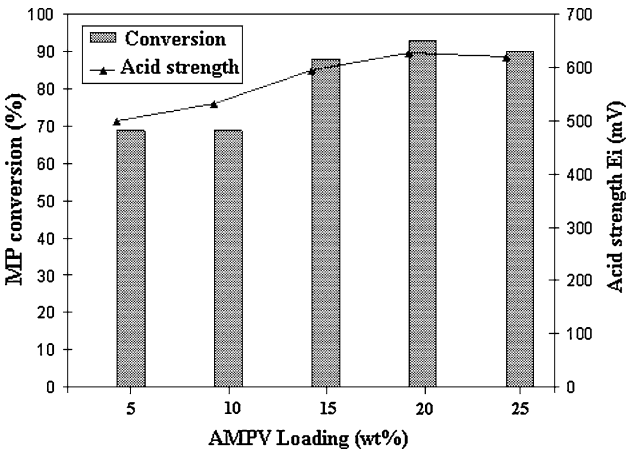

Fig. 6 Correlation between MP conversion and acid strength of AMPV/CeO_2 catalysts

The correlation between the conversion and the acid strength of the catalyst are shown in Fig. 6. The results suggest a good correlation between the acid strength and conversion of the catalysts. The 20wt% AMPV/CeO_2 catalyst showed maximum acidity and conversion. In ammoxidation reaction, conversion depends upon the acidity and whereas the selectivity depends on the redox properties, nature of support and reaction temperature.

4 Conclusions

The synthesis of AMPV with Keggin structure on CeO_2 support is achieved in a single step. The AMPV/CeO_2 catalysts are thermally more stable compared to the bulk AMPV catalyst. A maximum conversion and selectivity to CP was obtained on 20% AMPV/CeO_2 catalyst. The conversion of MP depends on the acid strength of the catalysts. The CeO_2 supported AMPV catalysts are more active and selective compared to other supports. The high activity and selectivity of CeO_2 supported catalysts may be due to the combination of vanadium (known for its redox properties) and CeO_2 (known for its oxygen storage and release functions).

Acknowledgments KMR thanks to CSIR, New Delhi for the SRF fellowship. The authors acknowledged to DST, New Delhi, for the financial support under their SERC scheme, DST No. SP/S1/H-25/2001.

References

1. Okuhara T, Mizuno N, Misono M (1996) Adv Catal 41:113
2. Kozhevnikov IV (1998) Chem Rev 98:171

3. Bonardet JL, Carr K, Fraissard J, McGarvey GB, McMonagle JB, Seay M, Moffat JB (1996) Microporous metal-oxygen cluster compounds (heteropoly oxometalates). In: Moser WR (ed) Advanced catalysts and nanostructured materials, modern synthetic methods. Academic Press, New York, p 395
4. Rocchioccioli-Deltcheff C, Aouissi A, Bettahar M, Launay S, Fournier M (1996) J Catal 164:16
5. Bruckman K, Tatibouet JM, Che M, Serwicka E, Haber J (1993) J Catal 139:455
6. Neumann R, Dror I (1998) Appl Cat A Gen 172:67
7. Liu H, Iglesia E (2003) J Phys Chem B 107:10840
8. Martin A, Lucke B (2000) Catal Today 7:61
9. Roy SK, Dutta P, Nandi LN, Yadav SN, Mondal TK, Ray SC, Mitra S, Samuel P (2004) J Mol Cat A Chem 223:211
10. Cavalli P, Cavani F, Manenti I, Trifiro F (1987) Catal Tod 1:245
11. Centi G (1996) Appl Cat A Gen 147:267
12. Centi G, Perathoner S, Trifiro F (1997) Appl Cat A Gen 157:143
13. Grasselli RK (1999) Catal Tod 49:141
14. Chary KVR, Praveen Kumar CH, Ramana Rao PV, Rao VV (2004) Catal Commun 5:479
15. Kanta Rao P, Rama Rao KS, Khaja Masthan S, Narayana KV, Rajiah T, Venkat Rao V (1997) Appl Cat A Gen 163:123
16. Feng T, Vohs JM (2004) J Catal 221:619
17. Burcham LJ, Deo G, Gao X, Wachs IE (2000) Top Cat 11/12:85
18. Bart JCJ, Giordano N (1982) J Catal 75:134
19. Villabrille P, Vazquez P, Blanco M, Caceres C (2002) J Colloid Interface 251:151
20. Massoth FE (1978) Adv Catal 27:265
21. Cousin R, Dourdin M, Aad EA, Courcot D, Capelle S, Guelton M, Aboukais A (1997) J Chem Soc Faraday Trans 93:3863
22. Matta J, Courcot D, Aad EA, Aboukaïs A (2002) Chem Mater 14:4118
23. Lingaiah N, Mohan Reddy K, Seshu Babu N, Narasimha Rao K, Suryanarayana I, Sai Prasad PS (2006) Catal Commun 7:245
24. Bernal S, Kasper J, Trovarelli A (1999) Catal Tod 50:173
25. Bardin BB, Davis RJ (1999) Appl Cat A Gen 185:283
26. Mohan Reddy K, Lingaiah N, Nagaraju P, Sai Prasad PS, Suryanarayana I (2008) Catal Lett 122:314
27. Bruckman K, Haber J, Serwicka EM, Yurichenko EN, Lazarenko TP (1990) Catal Lett 4:181
28. Marchal-Roch C, Laronze N, Villanneau R, Guillou N, Teze A, Herve G (2000) J Catal 190:173
29. Trovarelli A (1996) Cat Rev Sci Eng 38:439
30. Li XK, Zhao J, Ji WJ, Zhang ZB, Chen Y, Au CT, Han S, Hibst H (2006) J Catal 237:58
31. Spojakina AA, Kostova NG, Sow B, Stamenov MW, Jiratova K (2001) Catal Tod 65:315
32. Vazquez P, Pizzo L, Caceres C, Blanco M, Thomas H, Alesso E, Finkielsztein L, Lantano B, Moltrasio G, Aguirre J (2000) J Mol Catal A Chem 161:223
33. Forni L (1988) Appl Catal 37:305